Estimation of Total Atmospheric Ozone from GOES Sounder Radiances with High Temporal Resolution

JUN LI, CHRISTOPHER C. SCHMIDT, AND JAMES P. NELSON III

Cooperative Institute for Meteorological Satellite Studies, University of Wisconsin—Madison, Madison, Wisconsin

TIMOTHY J. SCHMIT AND W. PAUL MENZEL

Office of Research and Applications, NOAA/NESDIS, Madison, Wisconsin

(Manuscript received 8 November 1999, in final form 1 May 2000)

ABSTRACT

The potential for using Geostationary Operational Environmental Satellite (GOES) Sounder radiance measurements to monitor total atmospheric ozone is examined. A statistical regression using GOES Sounder spectral bands 1–15 radiances allows estimation of total atmospheric ozone. Hourly GOES ozone products have been generated since May 1998. GOES ozone estimates are compared with Total Ozone Mapping Spectrometer (TOMS) ozone measurements from the Earth Probe satellite and ground-based Dobson spectrometer ozone observations. Results show that the percentage root-mean-square (rms) difference between instantaneous TOMS and GOES ozone estimates ranges from 4% to 7%. Also, daily comparisons for 1998 between GOES ozone values and ground-based observations at Bismarck, North Dakota; Wallops Island, Virginia; and Nashville, Tennessee, show that the rms difference is approximately 21 Dobson units. Given the hourly measurements and high-spatial density provided by the GOES Sounder, GOES ozone estimates and associated products show promise.

1. Introduction

There has been much interest in atmospheric ozone in recent decades, due primarily to its role in complex mid-atmospheric photochemistry and the critical ecological effects associated with ozone depletion induced by anthropogenic impacts and natural processes. The evolution of the ''ozone hole'' and its interannual variability can be detected and even predicted by means of satellite observations. The main satellite instruments used for monitoring ozone are the Total Ozone Mapping Spectrometer (TOMS; Bowman and Krueger 1985; McPeters et al. 1996, 1998) and the Solar Backscatter Ultraviolet (SBUV) spectrometer (Heath et al. 1975, 1978). In order to predict the evolution of ozone on timescales of a few days to a week, reliable measurements of the three-dimensional distribution of ozone are needed. However, neither the TOMS nor the SBUV, which measure backscattered ultraviolet solar radiation, can provide measurements at night. Infrared (IR) radiance measurements, since they do not depend on backscattered solar energy, allow ozone estimates in regions of darkness. Other satellite instruments, such as the Global Ozone Monitoring Experiment (GOME; Burrows et al. 1999), the Microwave Limb Sounder (MLS; Waters et al. 1999), the Stratospheric Aerosol and Gas Experiment (SAGE; McCormick 1991), the Polar Ozone and Aerosol Measurement (POAM; Bevilacqua 1997), and the Halogen Occultation Experiment (HALOE; Russell et al. 1993) can also provide useful atmospheric ozone information.

Satellite-observed infrared radiances at 9.6 μm can be used to determine the global distribution of atmospheric ozone. Previous efforts in this area of research have used Television Infrared Observational Satellite (TIROS-N) Operational Vertical Sounder (TOVS; Smith et al. 1979) 9.6-μm radiances to retrieve total column ozone. Neuendorffer (1996) investigated TOVS ozone monitoring and applied TOVS ozone data to ozone hole detection. Engelen and Stephens (1997) compared their TOVS ozone retrievals with TOMS total ozone estimates and obtained agreement to within 10% rms for global-gridded TOVS measurements. Since April 1994, the new generation of Geostationary Operational Environmental Satellite (GOES; Menzel and Purdom 1994) Sounders have provided higher spatial and tem-

Corresponding author address: Dr. Jun Li, CIMSS/SSEC, Rm. 219, 1225 W. Dayton St., Madison, WI 53706.
E-mail: JunL@ssec.wisc.edu

TABLE 1. *GOES-8* Sounder noise performance. NEDR is the in-flight measured noise equivalent radiation in mW m^{-2} sr^{-1} cm^{-1}.

Wavelength (μm)	Band	NEDR (mW m^{-2} sr^{-1} cm^{-1})
14.7	1	1.63
14.4	2	1.41
14.1	3	0.94
13.9	4	0.65
13.4	5	0.74
12.7	6	0.32
12.0	7	0.21
11.0	8	0.15
9.7	9	0.20
7.5	10	0.091
7.0	11	0.091
6.5	12	0.119
4.57	13	0.012
4.52	14	0.011
4.45	15	0.012
4.13	16	0.004
3.98	17	0.005
3.7	18	0.002

poral resolution radiance measurements for deriving atmospheric parameters such as temperature and moisture (Menzel et al. 1998). Table 1 lists the *GOES-8* Sounder noise performance. NEDR is the in-flight measured noise equivalent radiation in mW m^{-2} sr^{-1} cm^{-1}. Included in its suite of 18 thermal infrared bands, all with approximately 10-km resolution, is a band sensitive to radiation near 9.7 μm (band 9). With *GOES-8*, *GOES-9*, and *GOES-10* 9.7-μm radiance measurements, ozone can be estimated on an hourly basis over virtually all of the continental United States and large portions of adjacent oceanic regions. As a result, GOES offers the first opportunity to investigate short timescale variations in the ozone distribution at the midlatitudes.

In this paper, an algorithm for estimating total atmospheric ozone and ozone profiles from GOES Sounder radiances is described. Ozone values derived from *GOES-8* radiance measurements between May 1998 and September 1999 are compared with time- and space-collocated TOMS ozone estimates and ground-based ozone observations from Bismarck, North Dakota; Wallops Island, Virginia; and Nashville, Tennessee.

2. Analysis of ozone information contained in the GOES ozone band radiance

GOES ozone band radiances contain atmospheric absorption, atmospheric radiation, and surface radiation information. The GOES ozone band also has high sensitivity to both atmospheric and surface skin temperatures as well as some sensitivity to absorption due to atmospheric moisture. Most importantly, the GOES ozone band exhibits moderate ozone absorption. In order to motivate the physical basis for ozone estimation from GOES Sounder measurements, the ozone information content of the GOES ozone band is examined through simulations.

If we neglect scattering by the atmosphere, the clear-sky radiance measured by the GOES satellite for a specific IR band within a field of view (FOV) is given by

$$R_i = \varepsilon_s B_s(T_s)\tau_s - \int_0^{p_s} B[T(p)]\, d\tau + (1 - \varepsilon_s)\int_0^{p_s} B[T(p)]\, d\tau^*, \quad (1)$$

where R_i is the clear-sky radiance for the ith spectral band as seen by the satellite sensor, $B[T(p)]$ is the Planck radiance, which is a function of the atmospheric temperature profile $T(p)$, and τ is the atmospheric transmittance, also a function of $T(p)$. The water vapor mixing ratio profile is denoted by $q(p)$ and the ozone mixing ratio profile by $O_3(p)$. The subscript s denotes surface values, τ^* is defined as $\tau^* = (\tau_s^2/\tau)$, ε_s is the surface emissivity, T_s is the surface skin temperature, and p_s is the surface pressure.

To linearize Eq. (1) the first-order variations $\delta B = (\partial B/\partial T)\partial T$ and $\partial R = (\partial R/\partial Tb)\partial Tb$ are used, the surface skin temperature and surface emissivity are assumed to be predetermined (Hayden 1988), and β is set to $\beta(p) = (\partial B/\partial T)/(\partial R/\partial Tb)$. The linearized form of Eq. (1) (Li 1994; Li et al. 2000) is

$$\delta \mathrm{Tb}_i = \int_0^{p_s} W_T \delta T\, dp + \int_0^{p_s} W_q \delta \ln q\, dp + \int_0^{p_s} W_{\mathrm{O}_3} \delta \ln \mathrm{O}_3\, dp, \quad (2)$$

where

$$W_T(p) = -\beta\frac{\partial \tau}{\partial p} + \beta(1 - \varepsilon_s)\frac{\partial \tau^*}{\partial p}, \quad (3a)$$

$$W_q(p) = \left[(T_s - T_a)\varepsilon_s\tau_s\beta_s - 2(1 - \varepsilon_s)\int_0^{p_s} \beta\tau^*\frac{\partial T}{\partial p}\, dp\right]\frac{\partial \ln\tau_q}{\partial p} + \left\{\int_p^{p_s} \beta[\tau + (1 - \varepsilon_s)\tau^*]\frac{\partial T}{\partial p}\, dp\right\}\frac{\partial \ln\tau_q}{\partial p}, \quad (3b)$$

$$W_{\mathrm{O}_3}(p) = \left[(T_s - T_a)\varepsilon_s\tau_s\beta_s - 2(1 - \varepsilon_s)\int_0^{p_s} \beta\tau^*\frac{\partial T}{\partial p}\, dp\right]\frac{\partial \ln\tau_{\mathrm{O}_3}}{\partial p} + \left\{\int_p^{p_s} \beta[\tau + (1 - \varepsilon_s)\tau^*]\frac{\partial T}{\partial p}\, dp\right\}\frac{\partial \ln\tau_{\mathrm{O}_3}}{\partial p}. \quad (3c)$$

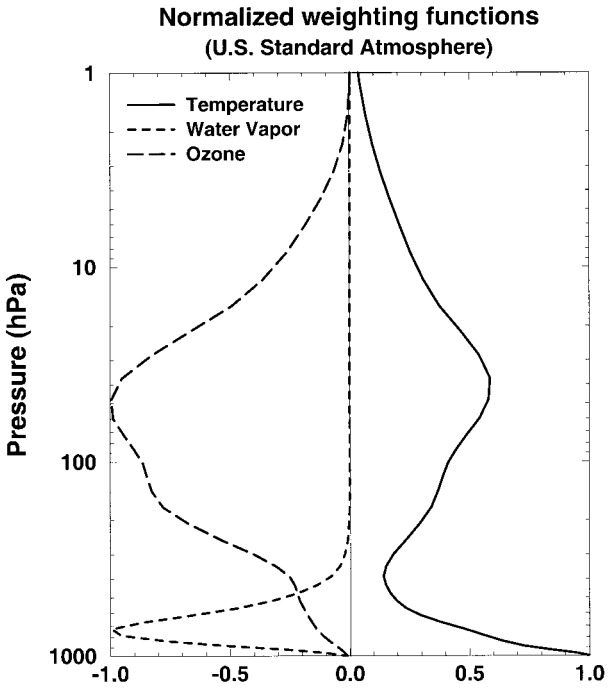

FIG. 1. The atmospheric temperature, water vapor and ozone mixing ratio (water vapor and ozone are expressed as the logarithm of the mixing ratio) component weighting functions for *GOES-8* ozone band.

Here Tb_i is the brightness temperature for the ith GOES Sounder band; τ_q and τ_{O_3} are the water vapor and ozone component transmittance functions, respectively; W_T, W_q, and W_{O_3} are the weighting functions (sensitivity functions) of the atmospheric temperature profile, water vapor mixing ratio profile, and ozone mixing ratio profile, respectively.

Figure 1 shows normalized weighting functions for the *GOES-8* ozone band with respect to atmospheric temperature, water vapor mixing ratio, and ozone mixing ratio for the *U.S. Standard Atmosphere.* Significant sensitivity to ozone is seen in the lower stratosphere and upper troposphere. Although the lower stratosphere contains only half of the total column ozone, it is responsible for the bulk of the ozone variability. Much of this variability is caused by a drop in the height of the tropopause or by stratospheric intrusions within a tropopause fold (Neuendorffer 1996). Since the GOES ozone band has less ozone sensitivity in the mid- and upper stratosphere, it is less capable of detecting the ozone variability in this region. The GOES ozone band is also sensitive to both surface and stratospheric temperatures, thus knowledge of atmospheric temperature is important so that the ozone information can be sorted out. The GOES ozone band is also affected by water vapor absorption with a moisture sensitivity peak at approximately 700 hPa.

To analyze the influence of atmospheric temperature and moisture on the ozone estimation from the GOES ozone band, a simple regression relationship is generated for total ozone estimation:

$$\mathrm{TOZ} = D_0 + D_1\mathrm{Tb}_9 + D_2\mathrm{Tb}_9^2 + E_0T_s + \sum_{i=1}^{L_s} E_iT_i + \sum_{i=1}^{L_s} F_i \ln q_i, \quad (4)$$

where TOZ is the total ozone value in Dobson units (DU); T_i and q_i are the atmospheric temperature and water vapor mixing ratio at pressure level p_i^{σ}, L_s denotes the surface level; and D, E, and F are the regression coefficients. Equation (4) quantifies the total ozone information available from the GOES ozone band radiance as well as accounting for additional atmospheric temperature, atmospheric moisture, and surface skin temperature information. The quadratic term approximates the nonlinear relationship between atmospheric ozone and GOES Sounder radiances. *GOES-8* ozone band radiances were simulated using Eq. (1) and 2631 global radiosonde profiles located between 10° and 60°N. Time- and space-collocated ground-based ozonesonde observations or satellite-based SBUV measurements are incorporated into these radiosonde profiles so that they contain atmospheric temperature, moisture, and ozone profiles. A fast atmospheric transmittance model, Pressure Layer Optical Depth (PLOD; Hannon et al. 1996), is used for the radiative transfer calculations. PLOD uses 42 vertical pressure level coordinates ranging from 0.1 to 1050 hPa. The *GOES-8* instrument noise of 0.20 mW m^{-2} sr^{-1} cm^{-1} (see Table 1) plus an assumed 0.2-K forward model error were added into the simulated *GOES-8* ozone band radiance. The regression coefficients were generated using 90% of the 2631 profiles (dependent samples). These coefficients were then applied to the remaining 10% of the profiles (independent samples) to get the percentage rms error (%rmse) of the total ozone estimate. Note that rmse is always used to indicate the error in simulation analysis since the retrieval can be evaluated against ''truth,'' while rms difference (rmsd) is used in real data validation.

The simulation study focused on the following three configurations [note that the regression coefficients in Eq. (4) are recomputed for each configuration].

1) The atmospheric temperature profile, surface skin temperature, and atmospheric moisture profile are assumed unknown in the regression by setting the regression coefficients E and F to zero in Eq. (4). Only the *GOES-8* ozone band radiance is used as predictor.
2) The atmospheric temperature profile and surface skin temperature are assumed unknown by setting the regression coefficient E to zero in Eq. (4), but the atmospheric moisture profile is assumed to be known. The water vapor mixing ratios are used as additional predictors in Eq. (4), and it is assumed

TABLE 2. The %rmse of total ozone estimates from simulated GOES ozone band radiances with water vapor error varies from 30% to 5%. The 245 independent samples are used in ozone %rmse calculation.

Atmospheric prior information	%rmse
T unknown; q unknown	11.26
T unknown; q known with 30% error	10.99
T unknown; q known with 25% error	10.89
T unknown; q known with 20% error	10.87
T unknown; q known with 15% error	10.73
T unknown; q known with 10% error	10.65
T unknown; q known with 5% error	10.05

TABLE 3. The %rmse of total ozone estimates from simulated GOES ozone band radiances with temperature error varies from 3.5 to 0.5 K. The 245 independent samples are used in ozone %rmse calculation.

Atmospheric prior information	%rmse
T unknown; q unknown	11.26
T known with 3.5-K error; q unknown	6.73
T known with 2.5-K error; q unknown	6.26
T known with 2.0-K error; q unknown	6.02
T known with 1.5-K error; q unknown	5.78
T known with 1.0-K error; q unknown	5.58
T known with 0.5-K error; q unknown	5.33

that the error for water vapor mixing ratios is constant at each pressure level. This configuration studies the impact of atmospheric moisture on the total ozone estimates by varying the moisture error from 5% to 30%.

3) The atmospheric temperature profile and surface skin temperature are assumed to be known, but the atmospheric moisture profile is assumed unknown by setting the regression coefficient F to zero in Eq. (4). The atmospheric and surface skin temperatures are used as additional predictors in Eq. (4), and it is assumed that the error for temperatures is also constant at each pressure level and for the surface skin. This configuration studies the impact of the atmospheric and surface skin temperatures on the total ozone estimation by varying the temperature error from 0.5 to 3.5 K.

Table 2 lists the %rmse of total ozone estimates from configurations 1 and 2. There is little sensitivity to moisture in the ozone estimation. The %rmse exhibits little change as water vapor error is reduced from 30% to 5%. The %rmse of ozone estimates from configuration 2 (with water vapor information available) is very close to that from configuration 1; it can be inferred that only a general a priori moisture profile is needed for GOES ozone estimates. Table 3 lists the %rmse of total ozone estimates from configuration 3 and those from configuration 1. There are large sensitivities to temperature in the ozone estimation. The %rmse decreases ~1.0% as the temperature error decreases from 3.5 to 1.5 K. The %rmse of total ozone estimates from configuration 3 is reduced significantly from that of configuration 1. Table 3 indicates that the %rmse of configuration 1 estimates can be as large as 11%, while the %rmse of configuration 3 estimates is 5%–6%. This strong correlation between atmospheric temperature and ozone estimates implies that a precise knowledge of atmospheric temperature improves the ozone rmse by approximately a factor of 2. This conclusion is also consistent with previous IR ozone retrieval studies summarized by Neuendorffer (1996) and other recent studies (Ravetta et al. 1999).

In order to investigate the influence of the GOES instrument noise on the ozone estimation, additional simulations for configuration 3 with the *GOES-8* nominal instrument noise adjusted by a noise factor (NF) were carried out. The NF was set to 2.0, 1.5, 1.0, 0.5, and 0.33, respectively. An error of 2.0 K was assumed for atmospheric and surface skin temperatures in the simulations. Table 4 lists the %rmse of total ozone estimates from simulated GOES ozone band radiances with different instrument noise factors. Overall, the instrument noise has some influence on the accuracy. Lower instrument noise could result in better ozone estimates.

3. Algorithm for ozone estimation from GOES spectral band radiances

Temperature and moisture profiles as well as the surface temperature can be inferred from a combination of GOES CO_2 spectral bands and water vapor bands. To account for the atmospheric temperature, moisture, and surface skin temperature effects, an empirical regression of GOES sounder radiances against ozone mixing ratio profiles is used. The current GOES ozone algorithm consists of the following expression:

$$\ln[O_3(p)] = A_0 + \sum_{j=1}^{15} A_j \mathrm{Tb}_j + \sum_{j=1}^{15} A'_j \mathrm{Tb}_j^2 + C_1 p_s + C_2 \sec\theta + C_3 \cos\left(\frac{M-6}{12}\pi\right) + C_4 \cos(\mathrm{LAT}), \quad (5)$$

where A, A', and C are the regression coefficients; θ is the local zenith angle of GOES FOV; M is the month from 1 to 12; LAT is the latitude of the GOES FOV; and j is the GOES band index. Since the logarithm of the water vapor mixing ratio or ozone mixing ratio shares a closer linear relation to the radiance than the

TABLE 4. The %rmse of total ozone estimates from simulated GOES ozone band radiances with differernt instrument noise factors.

Noise factor	%rmse
2.0	6.35
1.5	6.25
1.0	6.02
0.5	5.78
0.33	5.51

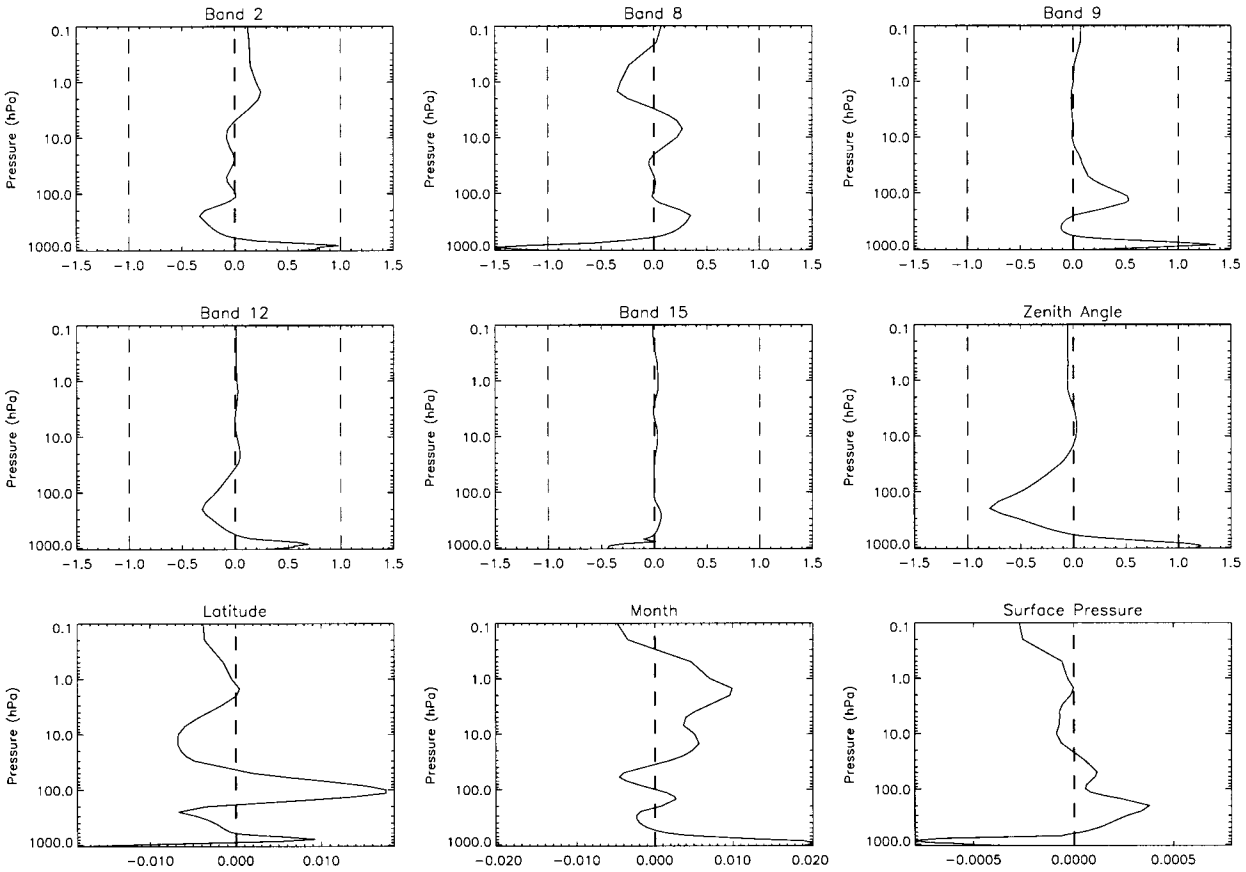

FIG. 2. The regression coefficients as a function of pressure for channels 2, 8, 9, 12, and 15, and additional predictors of zenith angle, latitude, month, and surface pressure.

mixing ratio does in the radiative transfer equation (Li et al. 2000), $\ln[O_3(p)]$ is used as the predictand in the regression. Fifteen GOES Sounder spectral band radiances are used as the primary predictors in the regression. Previous studies have shown that the accuracy of ozone estimates using 15 IR spectral bands is better than when using fewer spectral bands (Schmidt 2000). Month and latitude are included as additional predictors in the regression because midstratospheric ozone is a complex function of latitude, season, and temperature.

The 2631 profiles mentioned in section 2 were used to determine the regression coefficients. The radiative transfer calculation of *GOES-8* spectral band radiances using Eq. (1) is performed for each profile from the training dataset to provide an ozone profile/*GOES-8* radiance pair for use in the statistical regression analysis. The emissivity for the window band (*GOES-8* 11.03-μm spectral band) in the forward model calculation is assumed to be 0.98. The *GOES-8* Sounder instrument noise (Table 1) plus assumed 0.2-K forward model error is added into the calculated spectral band radiances. The regression equation [Eq. (5)] is then generated based on these calculated radiances and the matching ozone profile. To complete the regression, Eq. (5) can be applied to the GOES real-time measurements to obtain the estimated ozone profile, integration of which yields the total column ozone.

The regression coefficients reflect the relative contributions to the estimated ozone profile by the selected predictors. Figure 2 illustrates the regression coefficients as a function of pressure for bands 2, 8, 9, 12, and 15, and the additional predictors of zenith angle, latitude, month, and surface pressure. Each band has a distinct set of peaks indicating where it provides information about the ozone profile. Notably, the ozone band (9), has a single peak located near 200 hPa, a location consistent with providing information about the lower stratosphere and upper troposphere. All of these bands have some sensitivity to surface emissions. Relative to the other bands, band 15 does not contribute much information and therefore has little impact on the profile. Except for the zenith angle, the non-GOES Sounder predictors provide little additional ozone information (note that the scales for the last three predictors in Fig. 2 are very small).

Ozone estimation involves several steps, some of which are the same as those for temperature/moisture profile retrievals (Menzel et al. 1998): (a) identify clear versus cloudy FOVs by intercomparing brightness temperatures in adjacent CO_2 bands (Hayden 1988), (b)

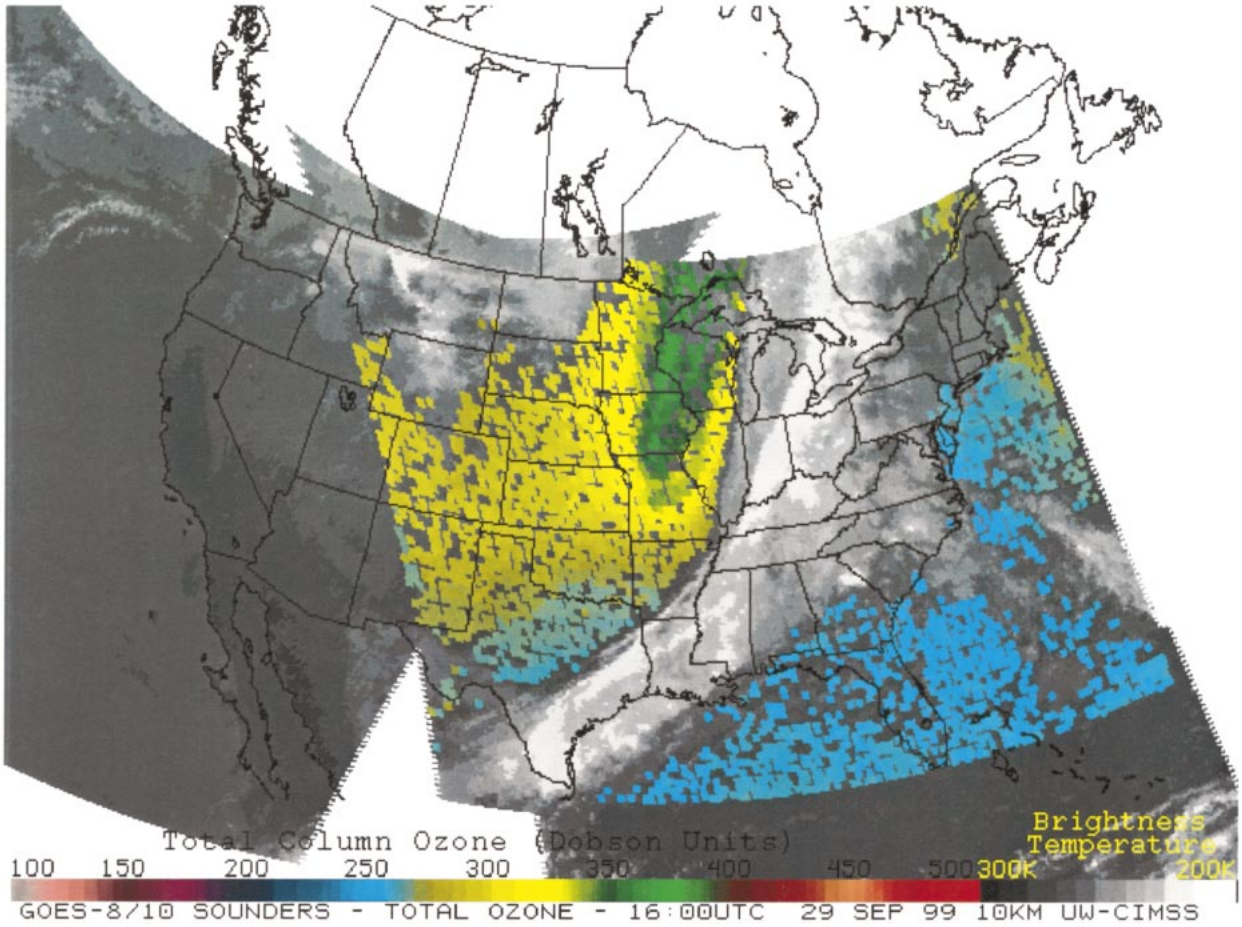

FIG. 3. The ozone map for 1600 UTC 29 Sep 1999. The units are in Dobson Units. The background image reflects the *GOES-8* and *GOES-10* window band brightness temperatures. Only *GOES-8* ozone estimates are shown.

average radiances for the clear-sky FOVs within a 3 by 3 FOV area (approximately 30 km on one side), and (c) apply a radiance bias adjustment (except to the ozone band). The 3 by 3 averaging reduces the radiance instrument noise and thus improves the accuracy of the product (see Table 4).

Figure 3 illustrates the coverage achieved on a randomly selected day and hour: 1600 UTC on 29 September 1999. Since the current retrievals are only done in regions determined to be cloud-free by a cloud-detection algorithm (Hayden 1988), the ozone retrievals only cover part of the sounder viewing area in this specific case. A large frontal system swept across the country during the previous 24 h and was associated with a lobe of enhanced ozone trailing behind the front.

4. Validation of GOES ozone estimates

Routine hourly GOES total ozone estimates have been generated since May 1998 at the Cooperative Institute for Meteorological Satellite Studies. TOMS level-2 ozone data (McPeters et al. 1998) have been collocated with GOES ozone estimates to within 1 h temporally and 0.25° spatially. The instantaneous comparisons are calculated in terms of percentage rmsd (%rmsd) between GOES and TOMS from May 1998 to September 1999. Figure 4 shows that the monthly %rmsd is less than 8% for all months in 1998 and 1999, with a minimum in the summer. From July to September the %rmsd is less than 5%, indicating good agreement between *GOES-8* and TOMS ozone estimates. Figure 5 shows a scatterplot of collocated *GOES-8* ozone estimates and TOMS ozone estimates for June 1998. Figure 6 shows the same for January 1999. *GOES-8* ozone estimates both in summer (Fig. 5) and in winter (Fig. 6) have good correlation with TOMS measurements, achieving correlation coefficients of 0.90 and 0.95 in June 1998 and January 1999, respectively. Figure 7 illustrates the distribution of differences between GOES and TOMS ozone estimates for four months between May 1998 and September 1999. The shapes of the peaks reflect the bias and scatter of the GOES ozone estimates relative to the TOMS ozone estimates. The peaks move from month to month, suggesting that the bias of GOES

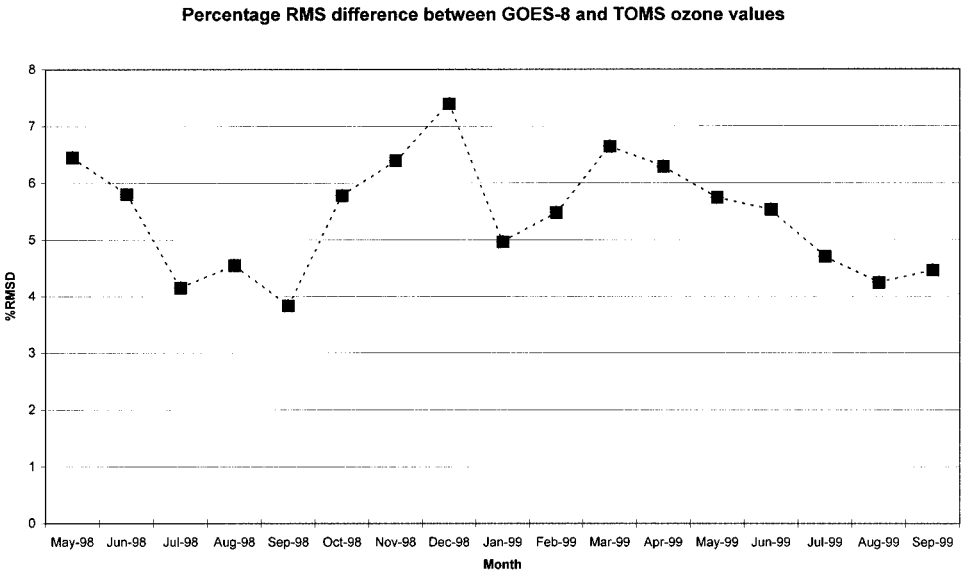

FIG. 4. The monthly %rmsd between the *GOES-8* ozone estimates and the TOMS ozone measurements between May 1998 and Sep 1999.

relative to TOMS ozone estimates depends on a variable or variables that have an annual cycle. The peak is widest in January and sharpest in July, indicating better consistency (less scatter) in the warmer months of the year than in the colder months. Although the scatter in winter is larger than in summer, the *GOES-8* ozone estimates capture the overall ozone variations well. Figure 8 shows the monthly mean ozone difference (TOMS minus *GOES-8*) from May 1998 to September 1999 and, like Fig. 7, also indicates that *GOES-8* underestimates the ozone values in summer but overestimates them in winter.

Figure 9 shows the %rmsd for different latitude zones in 1998 and 1999. It is apparent the %rmsd is larger in high latitudes than in lower latitudes. Overall, the agreement between GOES and TOMS ozone estimates is good in the region south of 40°N. Relatively large scatter (large %rmsd) in the region north of 40°N may be due to the comparatively larger ozone variation in this region. However, as illustrated in Fig. 10, GOES and TOMS ozone estimates in the band 45°–50°N continue to correlate well with a correlation coefficient of 0.95, despite a large scatter. Figure 11 shows zonal mean ozone differences between *GOES-8* ozone estimates and

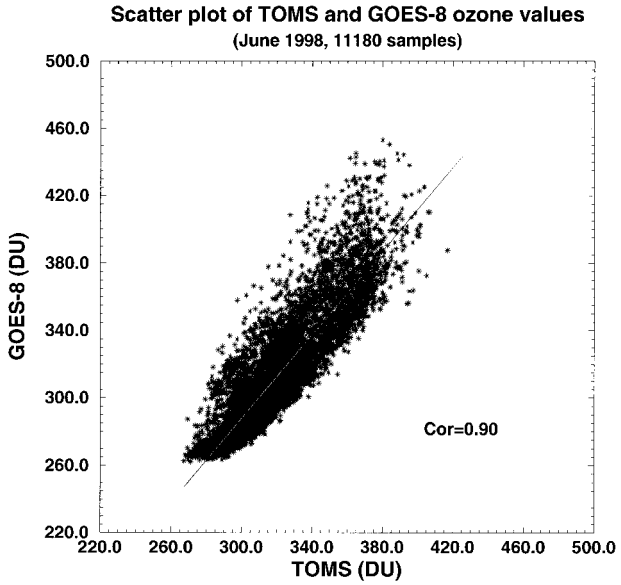

FIG. 5. Scatterplot of collocated *GOES-8* ozone estimates and the TOMS ozone measurements for Jun 1998.

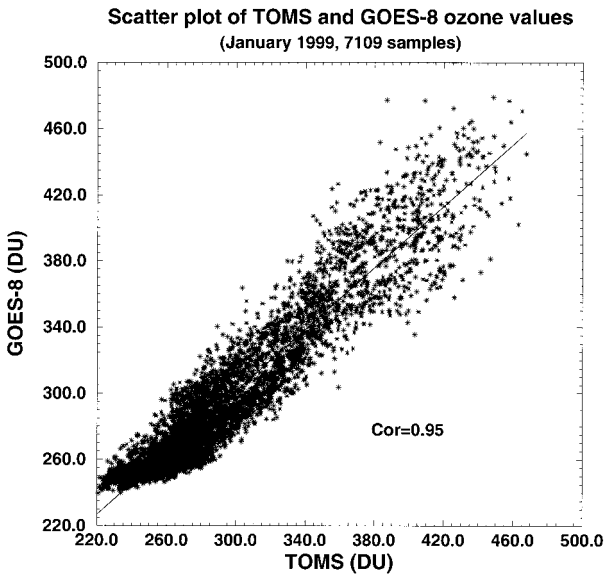

FIG. 6. Scatterplot of collocated *GOES-8* ozone estimates and the TOMS ozone measurements for Jan 1999.

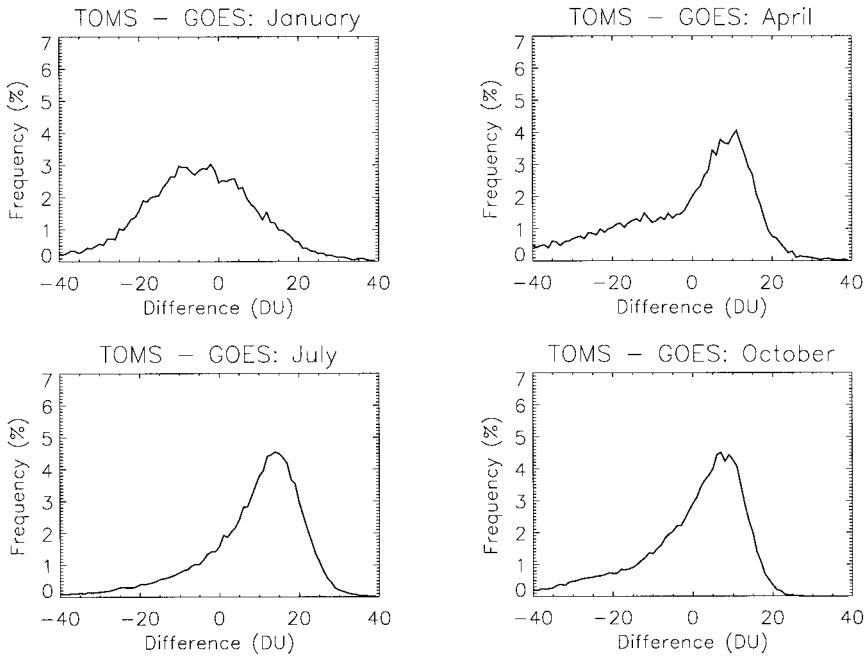

FIG. 7. Histograms outlining the scatter and differences between the GOES ozone estimates and TOMS ozone estimates in Jan 1999, Apr 1999, Jul 1999, and Oct 1998, capturing a 1-yr cycle.

TOMS ozone measurements (TOMS minus *GOES-8*) from May 1998 to September 1999. *GOES-8* underestimates the ozone values south of 40°N and overestimates the ozone values north of 40°N. The bias of GOES relative to TOMS is shown to vary from positive in the north to negative in the south, whereas the scatter (see Fig. 9) increases with increasing latitude.

To further quantify the quality of the *GOES-8* ozone estimates, single-site comparisons with ground-based Dobson–Brewer measurements (Komhyr et al. 1997) were performed at three locations in the continental United States for the period from May to December of 1998: Bismarck, North Dakota (46.77°N, 100.75°W), Nashville, Tennessee (36.25°N, 86.57°W), and Wallops Island, Virginia (37.87°N, 75.52°W). At each site, a daily ozone value was selected for *GOES-8*, TOMS, and ground-based total ozone observations. Only the *GOES-8* and TOMS ozone estimates closest to the ground-based observations in time and space were selected for the comparison. The time and space differ-

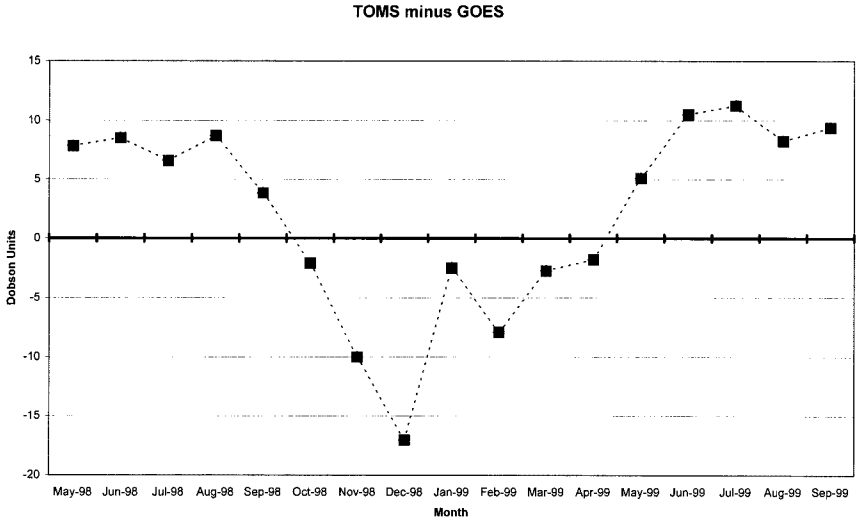

FIG. 8. The monthly mean ozone difference between the *GOES-8* ozone estimates and the TOMS ozone measurements (TOMS minus *GOES-8*) between May 1998 and Sep 1999.

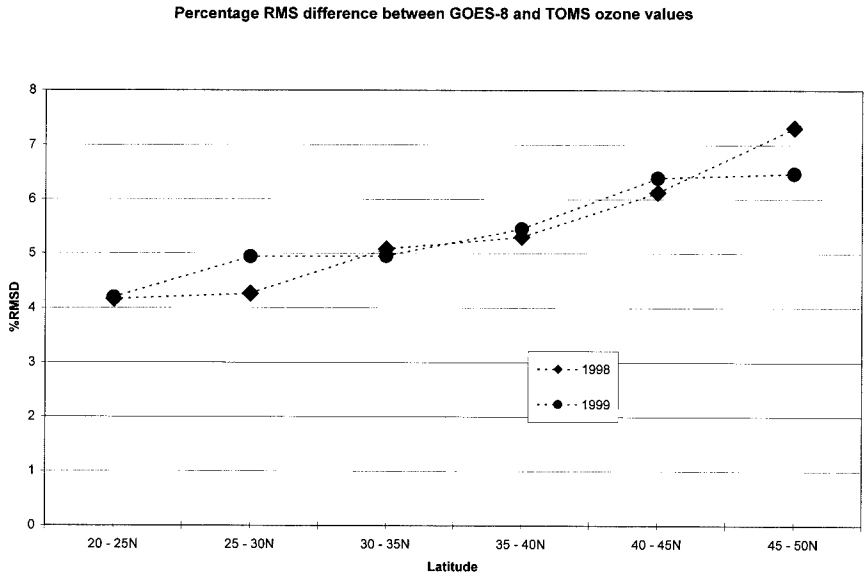

FIG. 9. The %rmsd between *GOES-8* ozone estimates and the TOMS ozone measurements for different latitude zones in 1998 and 1999.

ences among the three kinds of measurements may have had some influence on the comparisons. *GOES-8* total ozone estimates for Bismarck achieved an rmsd of 25 DU and a bias of −16 DU in 1998, while TOMS achieved a rmsd of 17 DU and a bias of −2 DU. GOES ozone estimates have a larger bias and rmsd than TOMS at Bismarck. This is consistent with larger GOES ozone estimate biases at higher latitudes, as indicated in Fig. 11. *GOES-8* total ozone estimates for Nashville have a bias of 1 DU and an rmsd of 17 DU, whereas TOMS has a bias of −8 DU and an rmsd of 17 DU. At Nashville, GOES performs better than TOMS with respect to bias and comparably with respect to rmsd. *GOES-8* total ozone estimates for Wallops Island had a bias of 6 DU and an rmsd of 21 DU, compared to a bias of −3 DU and an rmsd of 18 DU for TOMS at the same site. While at a similar latitude to the Nashville site, the *GOES-8* total ozone estimates achieved poorer performance at Wallops Island. This difference may be attributable to local variations in surface type within the 3 by 3 FOV area (land vs land and water).

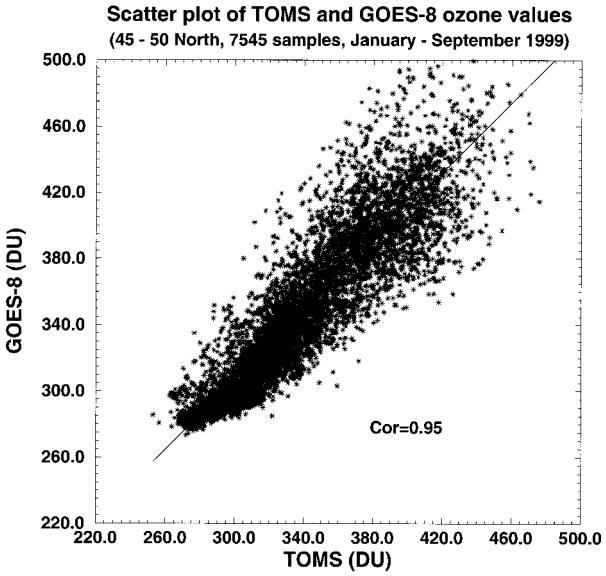

FIG. 10. The scatterplot of collocated *GOES-8* ozone estimates and the TOMS ozone measurements for 45°–50°N from Jan to Sep 1999.

Figure 12 contains a scatterplot of the *GOES-8* and TOMS total ozone estimates versus the surface-based ozone values at three locations. The GOES total ozone estimates show a similar scatter to that of the TOMS, as well as comparable biases (−2 DU for GOES and −4 DU for TOMS) and rmsd's (21 DU for GOES and 18 DU for TOMS) between the two instruments for this relatively small number of comparisons.

Hourly atmospheric ozone profile estimation is also possible using the regression algorithm presented in this study. Although there is only one GOES spectral band that has ozone absorption, an ozone profile can be estimated from the GOES Sounder measurements using the high correlation between the ozone profile and the temperature profile. Since the GOES Sounder provides hourly atmospheric brightness temperature measurements from which soundings are derived, ozone profile estimation becomes feasible. Validation of ozone profiles is difficult to carry out due to an insufficient number of collocated ozone profiles from ozonesondes and other satellites.

A simulation study to investigate the theoretical accuracy of ozone profile estimates was carried out. No forward model bias is assumed for the GOES ozone

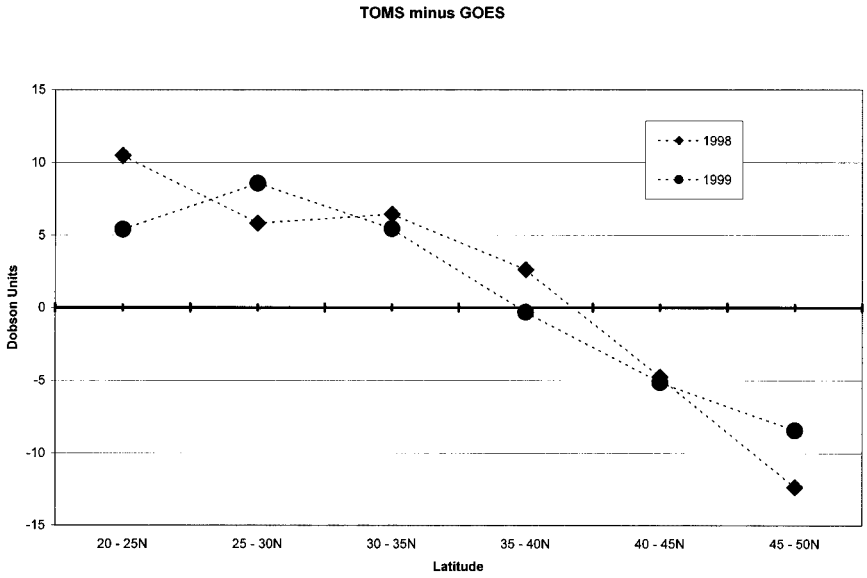

FIG. 11. Zonal mean ozone difference between the *GOES-8* ozone estimates and the TOMS ozone measurements (TOMS minus GOES) from May 1998 to Sep 1999.

band. The %rmse of the ozone mixing ratio profile is calculated from the independent samples. Figure 13 shows the mean ozone mixing ratio profile of the independent samples, along with the %rmse of the GOES ozone mixing ratio estimates from the independent samples at each pressure level. The accuracy for most mid- and upper-stratospheric ozone estimates is within 10% and only the upper-tropospheric ozone estimates exceed 15% error. This is encouraging since the highest atmospheric ozone concentration is above the upper troposphere and outside the region of highest error. Hourly ozone profiles are very useful in chemistry transport models and mesocale models, and are important in studies of the stratosphere–troposphere exchange (Ravetta et al. 1999).

Three factors outside of those discussed with the simulations in section 2 may have influenced the accuracy

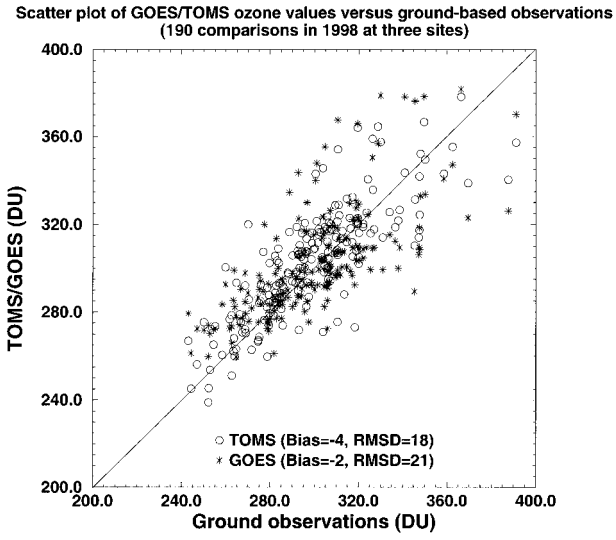

FIG. 12. Scatterplot of the *GOES-8* and TOMS total ozone estimates vs ground-based Dobson–Brewer measurements at three locations in the continental United States for the period from May to Dec of 1998: Bismarck (46.77°N, 100.75°W), Nashville (36.25°N, 86.57°W), and Wallops Island (37.87°N, 75.52°W).

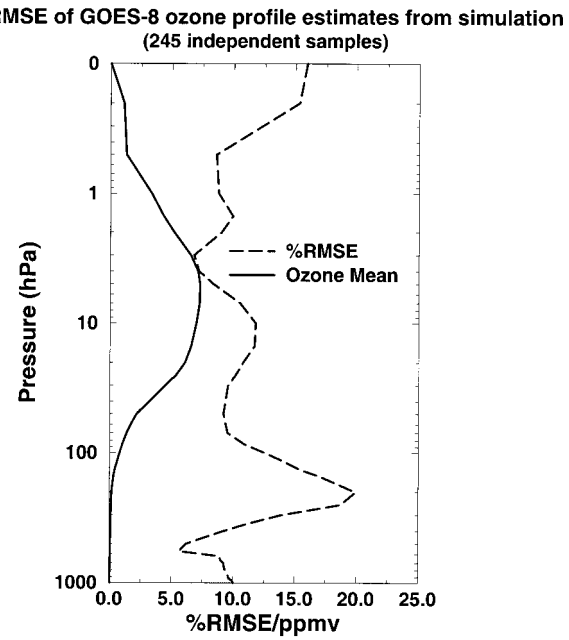

FIG. 13. A simulation study showing the mean ozone mixing ratio profile of the independent samples, along with the %rmse of the ozone mixing ratio estimates from the independent samples at each pressure level.

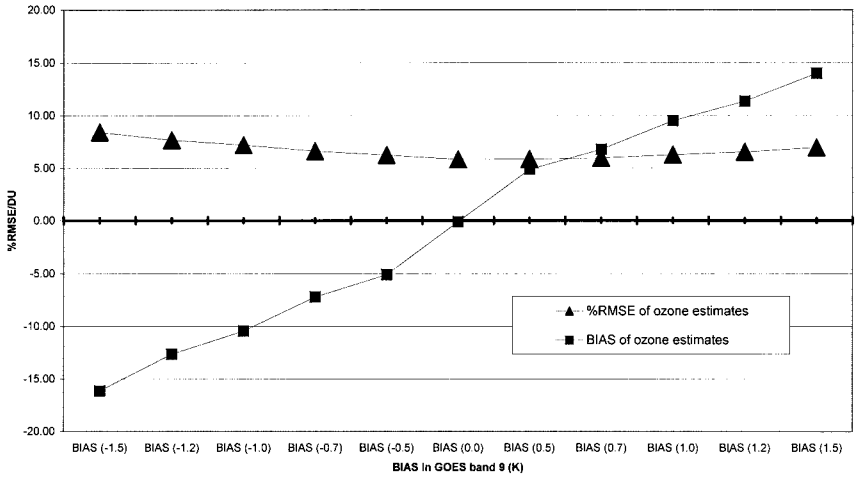

FIG. 14. A simulation study showing the %rmse and bias (true minus estimate) of the *GOES-8* ozone estimates from the independent samples with band 9 forward model bias varying from −1.5 to 1.5 K.

of GOES total column and profile ozone estimates. First, mid- and upper-stratospheric ozone variations in time and space will generate errors in the GOES ozone estimates since the ozone information content of the GOES ozone band radiance is focused on the lower stratosphere.

Second, an inadequate number of training profiles limits the accuracy of the GOES ozone estimates. To obtain reliable GOES ozone estimates, as many ozone profiles as possible for all four seasons from the latitudes covered by the GOES Sounder should be included in the training dataset. It is difficult to obtain a large number of time- and space-collocated ozone, temperature, and moisture profiles. In this paper, ground-based ozonesondes and satellite-based SBUV measurements were combined with time- and space-collocated temperature and moisture profiles to produce the training profile set. However, SBUV profiles in the lower stratosphere are influenced by the ozone climatology used in the SBUV retrievals. Other sources of ozone measurements such as SAGE, MLS, and POAM, which have plentiful ozone profile information with time- and space-collocated temperature and moisture profiles, will be considered for use in future versions of the GOES ozone estimation algorithm.

Finally, uncertainties associated with GOES Sounder spectral band forward model calculations (such as those due to inaccurate surface emissivity values, low-level cloud contamination, and surface elevation and type variations within the 3 by 3 FOVs) may bring additional error to the GOES ozone estimates. This is a potentially large error source. The forward model used here is a regression-based fast transmittance calculation model. Any bias or error in the forward model calculation will result in additional error in GOES total ozone estimation. To explore how the bias of the GOES ozone band forward model affects the ozone estimation, a simple simulation study was carried out to calculate the %rmse of GOES total column ozone estimates with model bias varying from −1.5 to 1.5 K. The 2631 temperature, moisture, and ozone profile trios are used in this simulation and the regression coefficients in Eq. (5) are generated using 90% of the 2631 profiles (dependent samples). These coefficients were then applied to the remaining 10% of the 2631 profiles (independent samples) to get the %rmse of the total ozone estimates. The noise added in the simulation is the *GOES-8* instrument noise. Figure 14 shows the %rmse and bias of the *GOES-8* total column ozone estimates from the independent samples with ozone band forward model bias varying from −1.5 to 1.5 K. Although the %rmse ranges from 5% to 9% when a forward model bias exists, the bias of the total ozone estimates resulting from the model bias ranges almost linearly from −15 to +15 DU as the model bias ranges from −1.5 to 1.5 K. Therefore, a large bias in the GOES ozone band forward model will produce a large bias in the GOES ozone estimates. Unlike the GOES Sounder CO_2 absorption bands, it is difficult to validate the GOES ozone band forward model and calculate the model bias due to insufficient GOES radiances collocated in time and space with atmospheric temperature, moisture, and ozone profiles, and thus no bias correction has been applied.

5. Conclusions

GOES ozone estimates from May 1998 to September 1999 show good agreement with TOMS ozone measurements; %rmsd ranges from 4%–7%. The comparison between GOES ozone estimates and ground-based ozone observations at three U.S. locations during 1998 indicates an rmsd of approximately 21 DU. The GOES Sounder spectral band radiances provide reasonable hourly ozone estimates of the total column atmospheric

ozone over North America and adjacent oceans in real time, providing for the first time a large regional database of short timescale ozone measurements.

Further work will extend the GOES Sounder ozone estimates to cloudy FOVs. More training data will be collected to improve the regression used for the GOES ozone estimates. Additional efforts will focus on the validation and improvement of the forward model for the GOES Sounder 9.7-μm spectral band. Once an accurate forward model for the GOES Sounder 9.7-μm spectral band is implemented, the ozone estimates can be further improved by using a physical iterative solution algorithm that is currently under development (Li et al. 1998). Also, the temporal or spatial distributions of ozone and their relationship to atmospheric dynamics, such as mesoscale vertical airmass exchange [clear-air turbulence (Shapiro 1999, personal communication)] will be investigated. Although all the results in this paper are from *GOES-8* measurements, the ozone estimates from other GOES satellite (e.g., *GOES-10*) have been obtained with the same algorithm on a limited basis. Furthermore, the general algorithm can be applied to any instrument that performs atmospheric temperature sounding and that has at least one ozone sensitive band. The GOES real-time hourly ozone estimates will continue to be collected for further study and application, and are available online at http://cimss.ssec.wisc.edu/goes/realtime/realtime.html.

Acknowledgments. The authors are grateful to Mr. George Stephens of NOAA/NESDIS for helping us access the TOMS level-2 data. Thanks are also due to Dr. Colin Seftor of Raytheon, STX Corporation, and Georgiann Batluck of the Ozone Processing Team (OPT) at NASA/GSFC, who respectively wrote and supplied the software to read in the TOMS data from its original format. The authors also gratefully acknowledge the contributions of the other members of the OPT. The ground-based ozone measurements were provided by Dorothy Quincy and Bob Evans of NOAA/ERL/CMDL. Three anonymous reviewers' comments were of considerable help in improving the text and clarifying some issues. This research is supported by NOAA Grant NA67 EC00100.

REFERENCES

Bevilacqua, R. M., 1997: Introduction to special section: Polar Ozone and Aerosol Measurement (POAM II). *J. Geophys. Res.,* **102,** 23 591–23 592.

Bowman, K. P., and A. J. Krueger, 1985: A global climatology of total ozone from the *Nimbus-7* total ozone mapping spectrometer. *J. Geophys. Res.,* **90,** 7967–7976.

Burrows, J. P., and Coauthors, 1999: The Global Ozone Monitoring Experiment (GOME): Mission concept and first scientific results. *J. Atmos. Sci.,* **56,** 151–175.

Engelen, R. J., and G. L. Stephens, 1997: Infrared radiative transfer in the 9.6-μm band: Application to TIROS operational vertical sounder ozone retrieval. *J. Geophys. Res.,* **102,** 6929–6939.

Hannon, S., L. L. Strow, and W. W. McMillan, 1996: Atmospheric infrared fast transmittance models: A comparison of two approaches. *Proc. SPIE,* **2830,** 94–105.

Hayden, C. M., 1988: GOES-VAS simultaneous temperature–moisture retrieval algorithm. *J. Appl. Meteor.,* **27,** 705–733.

Heath, D. F., A. J. Krueger, H. A. Roeder, and B. D. Henderson, 1975: The solar backscatter ultraviolet and total ozone mapping spectrometer (SBUV/TOMS) for NIMBUS G. *Opt. Eng.,* **14,** 323–331.

——, ——, and H. Park, 1978: The Solar Backscatter Ultraviolet (SBUV) and Total Ozone Mapping Spectrometer (TOMS) experiment. *The Nimbus-7 User's Guide,* C. R. Madrid, Ed., NASA Goddard Space Flight Center, 175–211.

Komhyr, W. D., G. C. Reinsel, R. D. Evans, D. M. Quincy, R. D. Grass, and R. K. Leonard, 1997: Total ozone trends at sixteen NOAA/CMDL and cooperative Dobson spectrophotometer observatories during 1979–1997. *Geophys. Res. Lett.,* **24,** 3225–3228.

Li, J., 1994: Temperature and water vapor weighting functions from radiative transfer equation with surface emissivity and solar reflectivity. *Adv. Atmos. Sci.,* **11,** 421–426.

——, J. P. Nelson, T. J. Schmit, W. P. Menzel, C. C. Schmidt, and H.-L. Huang, 1998: Retrieval of total atmospheric ozone from GOES sounder radiance measurements with high spatial and temporal resolution. *Proc. SPIE,* **3501,** 291–300.

——, W. Wolf, W. P. Menzel, W. Zhang, H.-L. Huang, and T. H. Achtor, 2000: Global soundings of the atmosphere from ATOVS measurements: The algorithm and validation. *J. Appl. Meteor.,* **39,** 1248–1268.

McCormick, M. P., 1991: SAGE III capabilities and global change. *29th Aerospace Sciences Meeting,* Paper 91-0051, Reno, Nevada, American Institute of Aeronautics and Astronautics, 8 pp.

McPeters, R. D., and Coauthors, 1996: *Nimbus-7* Total Ozone Mapping Spectrometer (TOMS) data products user's guide. NASA Reference Publication 1384, National Aeronautics and Space Administration, Washington, DC, 67 pp.

——, and Coauthors, 1998: Earth Probe Total Ozone Mapping Spectrometer (TOMS) data products user's guide. NASA Tech. Paper 206895, National Aeronautics and Space Administration, Washington, DC, 72 pp.

Menzel, W. P., and J. F. W. Purdom, 1994: Introducing GOES-I: The first of a new generation of geostationary operational environmental satellites. *Bull. Amer. Meteor. Soc.,* **75,** 757–781.

——, F. C. Holt, T. J. Schmit, R. M. Aune, A. J. Schreiner, G. S. Wade, and D. G. Gray, 1998: Application of *GOES-8/9* soundings to weather forecasting and nowcasting. *Bull. Amer. Meteor. Soc.,* **79,** 2059–2077.

Neuendorffer, A. C., 1996: Ozone monitoring with TIROS-N operational vertical sounders. *J. Geophys. Res.,* **101,** 18 807–18 828.

Ravetta, F., G. Ancellet, J. Kowol-Santen, R. Wilson, and D. Nedeljkovic, 1999: Ozone, temperature, and wind field measurements in a tropopause fold: Comparison with a mesoscale model simulation. *Mon. Wea. Rev.,* **127,** 2641–2653.

Russell, J. M., III, and Coauthors, 1993: The Halogen Occultation Experiment. *J. Geophys. Res.,* **98,** 10 777–10 797.

Schmidt, C. C., 2000: Hourly ozone estimation utilizing GOES I-M sounder. M.S. thesis, Department of Atmospheric and Oceanic Sciences, University of Wisconsin—Madison, 133 pp. [Available from Schwerdtfeger Library, 1225 W. Dayton St., Madison, WI 53706.]

Smith, W. L., H. M. Woolf, C. M. Hayden, D. C. Wark, and L. M. McMillin, 1979: TIROS-N operational vertical sounder. *Bull. Amer. Meteor. Soc.,* **60,** 1177–1187.

Waters, J. W., and Coauthors, 1999: The *UARS* and EOS Microwave Limb Sounder (MLS) experiments. *J. Atmos. Sci.,* **56,** 194–218.